Contents lists available at ScienceDirect

Biochemistry and Biophysics Reports

Psoriasis pathogenesis – Pso p27 constitutes a compact structure forming large aggregates

Hilde Lysvand [a], Ronny Helland [b], Lars Hagen [c], Geir Slupphaug [c], Ole-Jan Iversen [a,*]

[a] Department of Laboratory Medicine, Children's and Women's Health, Faculty of Medicine, Norwegian University of Science and Technology, NTNU, Postbox 8905, N-7491 Trondheim, Norway
[b] Department of Chemistry, Norwegian Structural Biology Centre, Faculty of Science and Technology, University of Tromsø, Tromsø, Norway
[c] Department of Cancer Research and Molecular Medicine, Faculty of Medicine and PROMEC Core Facility for Proteomics and Metabolomics, Norwegian University of Science and Technology, NTNU, Trondheim, Norway

ARTICLE INFO

ABSTRACT

Psoriasis is a chronic inflammatory skin disease. The absence of microbial organisms as potential causal agents has given rise to the hypothesis that the inflammation is due to an autoimmune reaction. The defined inflamed areas of the skin lesions argue for an immunological disease with a local production of a causal antigen. Pso p27 is a protein generated in mast cells in psoriatic plaques, but not in uninvolved skin. We recently demonstrated that the Pso p27 is generated by cleavage of SerpinB3 (SCCA1) in the presence of mast cell associated chymase.

In this communication we demonstrate by X-ray crystallographic analysis that the cleavage products associate into a complex similar to SCCA1, but with the reactive centre loop inserted into a 5-stranded central β-sheet.

Native gel electrophoresis show that these Pso p27 complexes form large aggregates which may be of significance with respect to an immunogenic role of Pso p27.

1. Introduction

Psoriasis is a chronic inflammatory skin disease that afflicts about 2% of the general population. Based on the fact that it has not been possible to identify an infectious causal agent it is postulated that psoriasis is an autoimmune disease. The confined psoriatic plaques indicate local production of an antigen, and that we are not dealing with a general failure in immunological tolerance of a common skin protein. The chronic nature of the inflammatory reaction indicates a positive feedback mechanism, implying that the inflammatory reaction contributes to its own maintenance.

Pso p27 is a protein which fulfils the criteria of an autoantigen in psoriasis [1,2]. It is present in mast cells in psoriatic plaques but not in healthy skin [3] and also in complement activating immune-complexes [1]. Based on sequence analysis of Pso p27 it was suggested that the protein is generated from post-translational processing of serpin-molecules [4]. Pso p27 and serpin-molecules are both present in mast cells in psoriatic lesions [5], and recently it was demonstrated that Pso p27 could be generated from recombinant SCCA1 (SerpinB3) with mast cell chymase [6]. The

cleavage reaction generates a core Pso p27 fragment identical to that found in psoriatic plaque as well as N-terminal and C-terminal minor fragments.

In this communication we present the X-ray crystallographic analyses of Pso p27 generated from chymase-treated SCCA1 and demonstrate that it appears with the N-terminal and C-terminal ends of SCCA1 as an integrated complex. The Pso p27-complex forms a more compact protein structure compared to the structure of SCCA1, with the reactive centre loop (RCL) inserted as an additional strand into the central β-sheet. The conformational shift is accompanied by a distinct shift in accessibility to antigenic epitopes in the protein and an increased propensity to form higher-order aggregates. Thus psoriasis may share common underlying molecular mechanisms with serpinopathies.

2. Materials and methods

2.1. Generation of protein extract from psoriatic plaques and affinity purification of Pso p27

Psoriatic scale (300 mg) was homogenized in 10 ml phosphate buffered saline (PBS) by using an UltraTurrax T25 (Rose Scientific

* Corresponding author. Fax: +47 72576416.
E-mail address: oleji@ntnu.no (O.-J. Iversen).

Ltd.). The crude extract was centrifuged at 16,000g for 10 min and 0.5 ml of the supernatant was applied onto a CnBr-activated Sepharose 4B column (GE Healthcare Life Sciences) coupled with monoclonal anti-Pso p27 antibodies. The column was eluted with 0.1 M glycine–HCl pH 2.6, 0.5 M NaCl. The purified Pso p27 was then neutralized, concentrated and desalted over a Nanosep 3K Omega spin filter (Pall Life Science).

2.2. Crystallization, X-ray data collection and structure determination

SCCA1 was expressed and purified as previously described [6]. To produce Pso p27, purified SCCA1 was incubated with human recombinant chymase (Sigma-Aldrich) at a ratio of 100:1 (w/w). The product was directly used for crystallization experiments. Initial crystallization trials of Pso p27 were conducted using an Art Robbins Phoenix crystallization robot to create 96-well crystallization setups using 60 μl in the reservoirs and 300 nl protein solution plus 300 nl reservoir solution in the experimental drops. Both commercial and homemade stochastic screens were tried. Crystallization conditions were found at both high and low pH; (1) 22% PEGMME 5K, 0.1 M Bicine pH 8.5, 0.06 M Zn acetate, 4.5% hexanediol and (2) 27% PEGMME 2K, 0.1 M Na acetate pH 4.5. X-ray diffraction data were collected at ID23-2 at the European Synchrotron Radiation Facility (ESRF) on crystals from both conditions. Data were integrated using XDS [7]. The structure was solved using MOLREP of the CCP4 software suite [8,9] using the structure of human squamous cell carcinoma antigen (SCCA1, PDB 2zv6 [10]) as template. Automatic re-tracing of the polypeptide chain was carried out with ARP/wARP [11]. Subsequent improvement of the model was made by alternate cycles of manual refitting of amino acids using Coot [12] based on sigma-weighted 2mFo-DFc and mFo-DFc electron density maps and refinement using Refmac5 [13] of the CCP4 suite. Illustrations of the crystal structure were prepared in PyMOL (Schrödinger, LLC; http://www.pymol.org)

2.3. Gel electrophoretic analyses

Samples were subjected to blue native polyacrylamide gel electrophoresis (BN-PAGE) in 4–16% NativePAGE Novex Bis-Tris gels using NativePAGE anode- and cathode buffers (Light blue). Denaturing SDS-polyacrylamide gel electrophoresis (SDS-PAGE) was performed in 4–12% NuPage Novex Bis-Tris gels using MOPS running buffer (Life Technologies). The gels were stained with Simply Blue Safe Stain (Life Technologies).

2.4. MALDI MS/MS analyses

Protein bands after both BN-PAGE and SDS-PAGE were in-gel digested using sequence grade modified trypsin (Promega) [14]. Peptides were extracted and desalted using StageTip purification [15]. Desalted peptides were mixed with 5 mg/ml HCCA in 50% CH$_3$CN, air-dried on a stainless steel sample stage and analysed on an Ultraflex III TOF/TOF (Bruker Daltonics) mass spectrometer.

2.5. Western blot analyses

After BN-PAGE, the gel was soaked in NuPAGE transfer buffer (Life Technologies) added 0.1% SDS for 1 h. Proteins were electro-blotted onto PVDF membranes using Bio-Rad Mini Trans-Blot Cell and NuPAGE transfer buffer for 1 h at 25 V. The membranes were blocked with 1% Blocking solution (Roche) in PBS and incubated with monoclonal antibody against Pso P27 [16,17] and anti-mouse horseradish peroxidase (HRP) conjugated secondary antibody (Dako) as described [5]. Finally 3,3-diaminobenzidine

tetrahydrochloride (DAB) (Sigma-Aldrich) was used as immunoblotting substrate.

3. Results

3.1. X-ray structure

Three dimensional crystals of approximate size $0.1 \times 0.05 \times 0.02$ mm^3 were obtained at both at high and low pH (8.5 and 4.5, respectively). The crystals diffracted to 2.15 Å and 2.0 Å, respectively, and belonged to the crystallographic space group $P2_12_12_1$ Data collection and refinement statistics is listed in Table 1.

The structures of Pso p27 at high and low pH could be solved by molecular replacement, identifying one molecule in the crystallographic asymmetric unit. The structure clearly identified Pso p27 as a complex with the N- and C-terminal peptides from SCCA1 (Fig. 1A). The polypeptide chains could be traced in electron density from residue 3 to 390 of the genetic sequence, with the exception of residues 65 to 79/80 (low and high pH, respectively) and residues 353–359. The folds of the high- and low-pH structures were almost identical, with an rms *xyz* displacement of 0.5 Å for main chain atoms, and only a minor difference in main chain conformation at residues 22–25. These residues are located on a solvent exposed surface site and they are not involved in crystal packing interactions. They are therefore not expected to affect putative interactions with other binding partners significantly, and hence in the following discussions the two structures will be

Table 1
Data collection and refinement statistics. Outer shell values are given in parenthesis.

|	High pH	Low pH
PDB code	4zk0	4zk3
Data collection		
Beam line	ESRF, ID 23-2	ESRF, ID 23-2
Diffraction limit (Å)	2.15	2.0
Space group	$P2_12_12_1$	$P2_12_12_1$
Outer shell values (Å)	2.22–2.15	2.05–2.00
Unit cell parameters		
a-axis (Å)	50.80	53.16
b-axis (Å)	68.27	68.84
c-axis (Å)	105.77	104.26
Total no. of reflections	133,216 (11,583)	175,871 (12,082)
No. of unique reflections	20,716 (1782)	26,612 (1964)
Completeness (%)	100 (100)	100 (100)
I/σ (I)	8.4 (1.5)	8.2 (1.2)
Mean I/σ (I)	15.9 (3.3)	14.9 (2.6)
R_{merge} (%)	7.9 (47.0)	7.8 (60.1)
Multiplicity	6.4 (6.5)	6.6 (6.2)
Wilson B (Å^2)	29.45	26.99
Refinement		
R_{work} (%)	17.44	18.11
R_{free} (%)	23.44	24.37
Average B factors (Å^2)	33.40	34.28
No. protein atoms	2979	2988
No. other atoms		
Solvent	111	187
Zn^{2+}	2	0
R.m.s. deviations		
Bond lengths (Å)	0.015	0.018
Bond angles (deg.)	1.706	1.819
% Residues in regions of the Ramachandran plot		
Most favoured	98.3	98.3
Additionally allowed	1.7	1.4
Outlier	0	0.3
DPI (based in Rfree)	0.2494 (20.36)	0.1857 (0.1760)
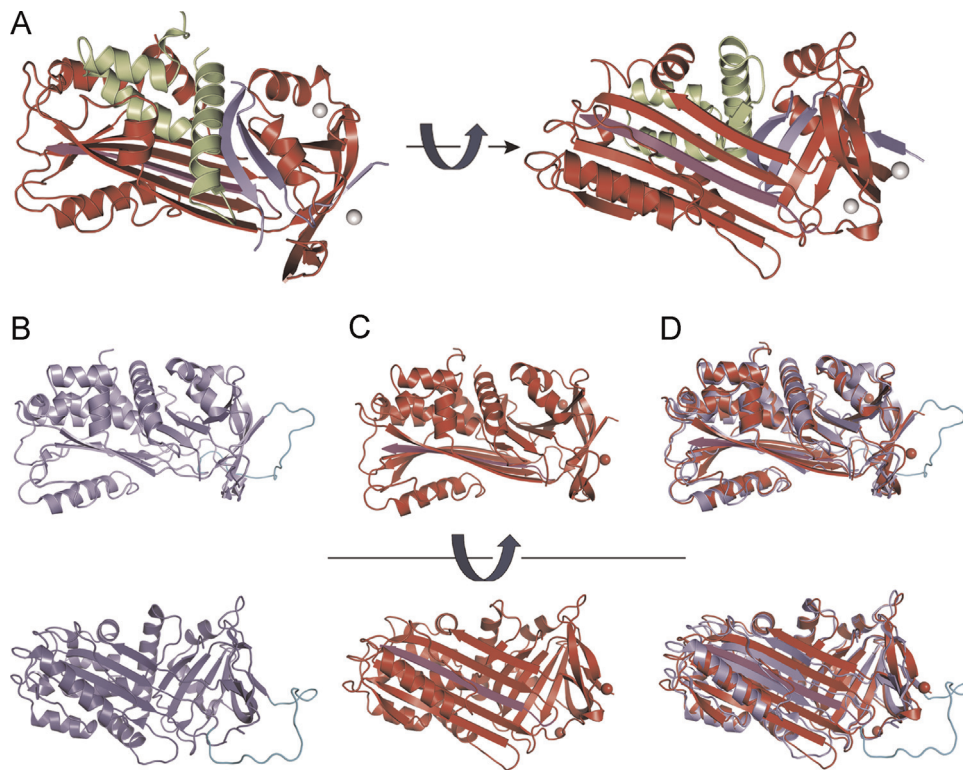
Fig.1. (A) Cartoon illustration of the Pso p27 complex at high pH. The core Pso p27 region is in red, with the the RCL loop (residues 338–352) inserted into the central β-sheet illustrated in magenta. The N-terminal cleavage fragment is in green and the C-terminal cleavage fragment is in blue. Grey spheres indicate the position of the metals found in the high pH structure. (B) Cartoon illustration of intact SCCA1 molecule B (PDB ID: 2ZV6, blue). The solvent exposed RCL (residues 340–359) is illustrated in cyan. (C) Cartoon illustration of the high pH Pso p27 structure (red). (D) Superimposition of Pso p27 and SCCA1.

considered identical. The structure of Pso p27 displays similarities to SCCA1, but in contrast to the structure deposited in the protein data bank (PDB 2ZV6 [10]) (Fig. 1B), where the central β-sheet consist of four strands and a solvent exposed reactive centre loop (RCL), the Pso p27 RCL is inserted between the parallel strands 2 and 3 of the central β-sheet. Similar structural rearrangement of intact serpins during protease inhibition has been described previously (reviewed in [18,19]). Molecules A and B in the deposited SCCA1 structure [10] differs primarily by molecule B having a solvent exposed reactive centre loop (RCL, residues 340–359), which is not traced in electron density in molecule A. Main chain atoms of Pso p27, excluding RCL residues 338–352 (Fig. 1C), could be superimposed on the corresponding residues of SCCA1 molecules A and B with rms *xyz* displacement values of about 1.7 Å (Fig. 1D, Fig. 2). The structural difference between Pso p27 and SCCA1 is primarily due the displacement of the four β-strands in order to accommodate the RCL between strands 2 and 3. The rest of the Pso p27 structure appears to be relatively unaffected by the insertion when compared to SCCA1. The structures reported here

are to higher resolution than the previously reported SCCA1 (2.0 and 2.15 Å vs. 2.7 Å [10]), and in addition to confirming burial of the RCL into the central β-sheet, our data suggests that Pso p27 is able to bind two metal ions. In the high pH structure, the metal is interpreted as Zn-ions since Zn was included in the crystallization conditions (Fig. 1A). In the low pH crystallization conditions, no metals were added. Still the electron density suggested that atoms heavier than water were present at the same sites as in the high pH structure.

3.2. SDS-page and BN-page

SDS-PAGE demonstrated similarity between Pso p27 generated from recombinant SCCA1 (Fig. 3A lane 3) and Pso p27 purified from scale extract by immunosorbent chromatography (Fig. 3A lane 5). In both instances a major band corresponding to monomeric Pso p27 (31.8 KDa) were observed. When the samples were subjected to analysis by BN-PAGE, bands corresponding to monomeric Pso p27 were not evident. However, three distinct
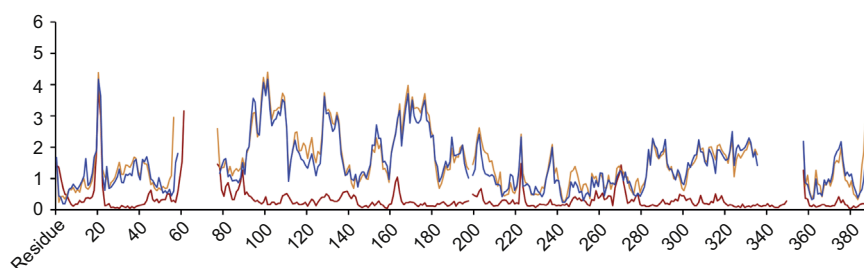

Fig. 2. Residual rms *xyz* differences in main chain atomic positions when comparing Pso p27 high pH structure (red), SCCA1 molecule A (orange) and SCCA molecule B (blue) to the low pH Pso p27 structure. The curves demonstrate the similarity of the two Pso p27 structures as well as structural differences between Pso p27 and SCCA1.
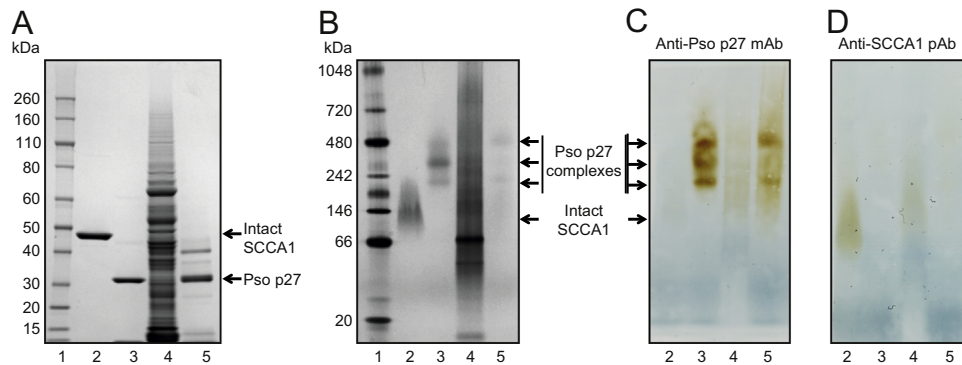
Fig. 3. Cleaved SCCA1 forms oligomeric Pso p27 complexes containing all three cleavage fragments, and that are antigenically distinct from intact SCCA1. (A) SDS-PAGE, (B) BN-PAGE, (C) Western analysis of BN-PAGE gel using anti-Pso p27 monoclonal antibody, (D) Western analysis of BN-PAGE gel using an anti-SCCA1 polyclonal antibody. Lane 1: protein MW standard (Novex Sharp Unstained Protein Standard for SDS-PAGE and Novex Native Mark Unstained Protein Standard for BN-PAGE), lane 2: intact recombinant SCCA1, lane 3: chymase-cleaved SCCA1, lane 4: psoriatic scale extract, and lane 5: immunosorbent-purified Pso p27 from scale extract.

bands in the range 200–450 KDa were observed with Pso p27 generated from recombinant SCCA1 (Fig. 3B Lane 3). A similar pattern of bands was observed with Pso p27 purified from scale extract (Fig. 3B lane 5). To further analyse the molecular composition of the higher-order complexes, bands were excised from both the recombinant and the immunosorbent samples, and tryptic peptides subjected to MS/MS analysis. The results demonstrated that each of the bands from both samples contained Pso p27 as well as the N- and C-terminal fragments from SCCA1. Thus the monomer constituents of the oligomeric Pso p27 complexes apparently resemble the cleaved SCCA1 observed in the crystallographic analysis. BN-PAGE of intact SCCA1 also indicated formation of a higher-order oligomer, but of considerably lower molecular mass than those observed with cleaved SCCA1 (Fig. 3B lane 2).

3.3. Western blot analysis

Western analysis subsequent to BN-PAGE, using monoclonal antibodies against Pso p27, demonstrated the presence of specific epitopes on the Pso p27-complexes (cleaved SCCA1) (Fig. 3C Lane 3) that were not detectable in intact SCCA1 (Fig. 3C Lane 2). This corroborates the crystallographic analyses, demonstrating that cleavage of SCCA1 mediates a marked conformational change with inclusion of the RCL into the central β-sheet (Fig. 1). The antigenic epitope was also evident in the Pso p27 complexes isolated from psoriatic scale extract (Fig. 3C, Lane 4). Conversely, when the blots were probed with polyclonal rabbit antibodies against the N-terminal end of SCCA1, a marked signal was observed over intact SCCA1 (Fig. 3D Lane 2), while no signal was observed over the Pso p27-complexes (Fig. 3D Lane 3).

4. Discussion

We have previously shown that SCCA1 is cleaved into three fragments by mast cell chymase, and that the major fragment corresponding to the core SCCA1 region is identical to Pso p27 isolated from psoriatic scale [6]. Here we demonstrate by X-ray crystallographic analysis that the cleavage products associate into a complex similar to SCCA1, but with a 5-stranded central β-sheet, instead of the 4-stranded sheet found in SCCA1. The fifth strand is formed by the reactive centre loop residues 338–352, which is inserted in an antiparallel manner between the parallel strands 2 and 3 in SCCA1. This feature is similar to what is observed in other serpins subsequent to binding and inhibition of their target substrates. The general mechanism of serpin inhibition

encompasses docking of the RCL loop into the active site of a target protease and formation of an productive Michaelis complex. This involves cleavage of the RCL, formation of a covalent bond between the protease and the P1 residue of the cleaved RCL and insertion of the RCL loop into the main β-sheet accompanied by translocation of the inactivated protease to the opposite pole of the serpin [19]. This conformational change in the serpin can also occur in the absence of substrate binding, and is driven by a large free energy difference between the active metastable state and the extended β-sheet state [20]. This also makes serpins containing point mutations susceptible to misfolding, polymerization and thereby causing various pathological conditions.

In SCCA1, inhibition of the target protease involves cleavage of the RCL loop between G357 and S354, mediating an ester bond between S354 and the protease. This is distinct from the chymase-induced cleavage mediating formation of Pso p27 from SCCA1, which occurs four residues N-terminal to G357, between V349 and V350. Moreover, we do not observe generation of covalent intermediates between cleaved SCCA1 and the chymase, as evident from SDS-PAGE analysis (Fig. 3A). It is thus likely that cleavage of the RCL between V349 and V450 is sufficient for its insertion into the central β-sheet and formation of a more stable conformational state.

The Pso p27 complex packs relatively tightly in the crystal with a solvent content of about 60% and crystallizes at both high and low pH, suggesting that it relatively easily may form ordered aggregates. A previous model of serpin polymerization hypothesizes that point mutations may induce *trans*-insertion of the RCL into the central β-sheet of another serpin (loop-sheet model), potentially forming larger aggregates [19]. However, crystal structures of mutated forms of antithrombin and antitrypsin (α1AT) indicate that polymerization rather occurs via *trans*-insertion of both the RCL and a central β-strand into a neighbouring molecule (domain swapping model) [21]. To what degree the soluble Pso p27 oligomers observed in BN-PAGE resemble the conformation observed in the crystals or whether *trans*-insertion of the RCL is involved presently remains elusive. Furthermore the role of metal ion binding in oligomerization remains to be established.

The concomitant presence of serpin-molecules and Pso p27 in mast cells in psoriatic plaques made us postulate that the translational modification from serpin-molecules to Pso p27 takes place in these cells [4–6]. MS/MS analyses of the bands shown in the BN-PAGE of Pso p27 (Fig. 3B) demonstrated the presence of the N- and C-terminal fragments from SCCA-molecules together with Pso p27. This observation together with the finding that the polyclonal antiserum against the N-terminal end of SCCA1 did not give any signal in Western analyses (Fig. 3, Lane 3) make us suggest that the

Pso p27 complexes are present as aggregates in an organized form. Based on the data presented it is reasonable to hypothesize that Pso p27 is present as an aggregated Pso p27-complex also inside the mast cells. The presence of subcellular, virus-like particles in psoriatic lesions, have been described previously [22], and analyses of isolated particles revealed membrane coated particles containing three core proteins with molecular weights estimated to 27, 15 and 12 kD, respectively, subsequent to denaturing size-exclusion chromatography [23,24]. It is thus tempting to speculate whether these virus-like particles represent aggregates of Pso p27-complexes released from mast cells though a budding process. It could be argued that this probably is an epiphenomenon associated with the disease. Based on the Western blot analysis described in this communication and immunofluorescence analysis [5,6] it seems obvious that the posttranslational modification of SCCA1 give rise to unique epitopes on the Pso p27-complex.

The high concentrations of Pso p27 specific antibodies extractable from psoriatic scale show that Pso p27 acts as an immunogen [25,26], and the presence of these antibodies in complement-activating immune complexes [1] suggest that Pso p27 plays a significant role in the inflammatory reactions in the psoriatic skin lesions.

Acknowledgements

Appendix A. Supplementary material

Supplementary data associated with this article can be found in the online version at http://dx.doi.org/.10.1016/j.bbrep.2015.06.001

References

[1] K. Asbakk, K. Bergh, O.J. Iversen, The psoriasis-associated antigen, pso p27, participates in the formation of complement activating immune-complexes in psoriatic scale, APMIS: Acta Pathol. Microbiol. Immunol. Scand. 98 (1990) 143–149.
[2] O.J. Iversen, K. Bergh, H. Lysvand, Use of scale antibodies for the detection of antigens in psoriatic lesions, Acta Derm.-Venereol. 73 (1993) 31–34.
[3] O.J. Iversen, H. Lysvand, T. Jacobsen, K. Bergh, B.A. Lie, The psoriasis-associated antigen, pso p27, is expressed by tryptase-positive cells in psoriatic lesions, Arch. Dermatol. Res. 287 (1995) 503–505.
[4] O.J. Iversen, H. Lysvand, L. Hagen, The autoantigen Pso p27: a post-translational modification of SCCA molecules, Autoimmunity 44 (2011) 229–234.
[5] O.J. Iversen, H. Lysvand, The autoantigen Pso p27 is generated from SCCA molecules in psoriatic plaques, WebmedCentral Dis. Mech. 3 (2012) 2–7.
[6] H. Lysvand, L. Hagen, L. Klubicka, G. Slupphaug, O.J. Iversen, Psoriasis pathogenesis-Pso p27 is generated from SCCA1 with chymase, Biochim. Biophys. Acta 1842 (2014) 734–738.
[7] W. Kabsch, Acta Crystallogr. Sect. D: Biol. Crystallogr. 66 (2010) 125–132.
[8] A. Vagin, A. Teplyakov, MOLREP: an automated program for molecular replacement, J. Appl. Cryst. 30 (1997) 1022–1025.
[9] M.D. Winn, C.C. Ballard, K.D. Cowtan, E.J. Dodson, P. Emsley, P.R. Evans, R. M. Keegan, E.B. Krissinel, A.G. Leslie, A. McCoy, S.J. McNicholas, G. N. Murshudov, N.S. Pannu, E.A. Potterton, H.R. Powell, R.J. Read, A. Vagin, K. S. Wilson, Overview of the CCP4 suite and current developments, Acta Crystallogr. Sect. D: Biol. Crystallogr. 67 (2011) 235–242.
[10] B. Zheng, Y. Matoba, T. Kumagai, C. Katagiri, T. Hibino, M. Sugiyama, Crystal structure of SCCA1 and insight about the interaction with JNK1, Biochem. Biophys. Res. Commun. 380 (2009) 143–147.
[11] A. Perrakis, R. Morris, V.S. Lamzin, Automated protein model building combined with iterative structure refinement, Nat. Struct. Biol. 6 (1999) 458–463.
[12] P. Emsley, B. Lohkamp, W.G. Scott, K. Cowtan, Features and development of Coot, Acta Crystallogr. Sect. D: Biol. Crystallogr. 66 (2010) 486–501.
[13] G.N. Murshudov, A.A. Vagin, E.J. Dodson, Refinement of macromolecular structures by the maximum-likelihood method, Acta Crystallogr. Sect. D: Biol. Crystallogr. 53 (1997) 240–255.
[14] A. Shevchenko, M. Wilm, O. Vorm, M. Mann, Mass spectrometric sequencing of proteins silver-stained polyacrylamide gels, Anal. Chem. 68 (1996) 850–858.
[15] J. Rappsilber, M. Mann, Y. Ishihama, Protocol for micro-purification, enrichment, pre-fractionation and storage of peptides for proteomics using Stage-Tips, Nat. Protoc. 2 (2007) 1896–1906.
[16] M. Dalaker, T. Jacobsen, H. Lysvand, O.J. Iversen, Expression of the psoriasis-associated antigen, Pso p27, is inhibited by cyclosporin A, Acta Derm.-Venereol. 79 (1999) 281–284.
[17] P. Song, H. Lysvand, Y. Yuhe, W. Liu, O.J. Iversen, Expression of the psoriasis-associated antigen, Pso p27, is inhibited by traditional Chinese medicine, J. Ethnopharmacol. 127 (2010) 171–174.
[18] G.A. Silverman, J.C. Whisstock, S.P. Bottomley, J.A. Huntington, D. Kaiserman, C. J. Luke, S.C. Pak, J.M. Reichhart, P.I. Bird, Serpins flex their muscle: I. Putting the clamps on proteolysis in diverse biological systems, J. Biol. Chem. 285 (2010) 24299–24305.
[19] J.C. Whisstock, G.A. Silverman, P.I. Bird, S.P. Bottomley, D. Kaiserman, C.J. Luke, S.C. Pak, J.M. Reichhart, J.A. Huntington, Serpins flex their muscle: II. Structural insights into target peptidase recognition, polymerization, and transport functions, J. Biol. Chem. 285 (2010) 24307–24312.
[20] H. Im, H.Y. Ahn, M.H. Yu, Bypassing the kinetic trap of serpin protein folding by loop extension, Protein Sci.: A Publ. Protein Soc. 9 (2000) 1497–1502.
[21] M. Yamasaki, T.J. Sendall, M.C. Pearce, J.C. Whisstock, J.A. Huntington, Molecular basis of alpha1-antitrypsin deficiency revealed by the structure of a domain-swapped trimer, EMBO Rep. 12 (2011) 1011–1017.
[22] A.B. Dalen, L. Hellgren, O.J. Iversen, J. Vincent, A virus-like particle associated with psoriasis, Acta Pathol. Microbiol. Immunol. Scand. Sect. B Microbiol. 91 (1983) 221–229.
[23] O.J. Iversen, A.B. Dalen, Urine proteins cross-reacting with antiserum against virus-like particles from cultured psoriatic epithelial cells, Acta Pathol. Microbiol. Immunol. Scand. Sect. B Microbiol. 91 (1983) 343–349.
[24] O.J. Iversen, Isolation of virus-like particles in urine from a psoriatic patient, Acta Pathol. Microbiol. Immunol. Scand. Sect. B Microbiol. 91 (1983) 407–412.
[25] O.J. Iversen, E. Rodahl, A.B. Dalen, Rabbit antibodies against the major internal protein of a retrovirus-like particle bind to epidermal cells in psoriatic skin. Brief report, Arch. Virol. 86 (1985) 341–346.
[26] O.J. Iversen, T. Jacobsen, Chronic Inflamm. Dis., Sarcoidosis, Vasc. Diffus. Lung Dis.: Off. J. WASOG/World Association of Sarcoidosis and Other Granulomatous Disorders 13 (1996) 66–69.